Ideal-Fluid Thermocline with Weakly Convective Adjustment in a Subpolar Basin*

RUI XIN HUANG

Department of Physical Oceanography, Woods Hole Oceanographic Institution, Woods Hole, Massachusetts

(Manuscript received 2 July 1987, in final form 3 November 1987)

ABSTRACT

The ideal-fluid thermocline with continuous stratification is extended to include a weakly convective adjustment process taking place in a subpolar basin. The convective adjustment creates a well-mixed layer on top of a moving unventilated thermocline where potential vorticity is specified as a boundary condition. Convective adjustment makes the moving water stratum shallower and the current more surface-intensified.

1. Introduction

The structure of the wind-driven circulation in a continuously stratified ocean has been a classic problem for almost 30 years. Welander (1959) first formulated a theory of the ideal-fluid thermocline. Ideal-fluid thermocline theory neglects all mixing/diffusion in the interior ocean and thus presents the simplest flow pattern for the interior ocean in which water particles conserve their density, Bernoulli function and potential vorticity as they enter the ocean's interior from all lateral boundaries.

Robinson and Stommel (1959) also presented a theory for the thermocline and thermohaline structure. Their theory emphasized the role of mixing.

During the past three decades, the concept of the ideal-fluid thermocline has been favored by theoretical oceanographers due to its simplicity. Because the inclusion of mixing makes the thermocline analytically difficult to handle, studies with mixing processes have mostly been carried out by numerical methods.

Welander (1971) took the second step in developing the ideal-fluid thermocline by suggesting that the problem might be solved by turning the original high-order partial differential equation into a second-order ordinary differential equation. He studied some simple analytical examples in which the form of the potential vorticity was specified.

A major difficulty in his approach is that the solutions obtained cannot satisfy all boundary conditions. Since a second-order ordinary differential equation can satisfy only two boundary conditions, it was obscure how to find solutions which satisfy the many boundary conditions imposed by a basin-scale model. He chose to satisfy the density condition on the upper surface and at the deep ocean, and thus left the Ekman pumping condition unsatisfied.

During the past five years, thermocline theory has evolved rapidly. Rhines and Young (1982) posed a theory of potential vorticity homogenization for the unventilated thermocline. Luyten et al. (1983) posed a theory for the ventilated thermocline. Pedlosky and Young (1983) studied semi-continuously stratified models for the thermocline. All these theories have given rise to new understanding of the thermocline structure. However, no truly continuous solution has been found. Huang (1986) extended Welander's (1971) solution to satisfy the Ekman pumping condition and obtained a three-dimensional continuous solution in a basin. Suitable boundary value problems for the ideal-fluid thermocline were still unknown.

Recently, Huang (1988a, H hereafter) has formulated deterministic boundary value problems for the ideal-fluid thermocline. Determining a solution of the high-order partial differential equation has been reduced to repeatedly solving some free boundary value problems for a second-order ordinary differential equation. The model provides a simple way of obtaining three-dimensional continuous solutions for the wind-driven gyres in a basin.

A major deficiency of the ideal-fluid thermocline is that the interior ocean is totally isolated from the mixed layer. In the original formulation of the ideal-fluid thermocline, the mixed layer plays only a passive role, that is to pump water down with specified density in a subtropical gyre and pick up water in a subpolar gyre.

For a more realistic model, the interaction between the mixed layer and the interior flow should be included. Pedlosky and Young (1983) studied a model for the subpolar basin. In the upper part of the ocean the isopycnals were vertical. Since no interaction with

* Contribution No. 6482 from the Woods Hole Oceanographic Institution.

Corresponding author address: Dr. Rui Xin Huang, Woods Hole Oceanographic Institution, Woods Hole, MA 02543.

the mixed layer was discussed in the model, they concluded that the model was underdetermined. This underdeterminate feature can be removed by introducing the convective adjustment process.

Our goal is to develop a model for the ideal-fluid thermocline with continuous stratification in a subpolar basin which includes the convective adjustment. The model is described in the next section. First, we derive all basic equations in density coordinates. Second, a boundary value problem of the ideal-fluid thermocline with weak convective adjustment is formulated for the case when the stagnant abyssal water is linearly stratified and potential vorticity is uniform for all of the unventilated thermocline; the problem is reduced to an analytical solution. (A boundary value problem for the general cases of nonuniform potential vorticity is briefly discussed in the Appendix.) A numerical example is presented in section 3 illustrating the homogenized water column and density fronts generated by convective adjustment. Finally, the conclusions are drawn in the last section.

2. Model formulation

The model ocean consists of a subpolar gyre in a rectangular basin on a β-plane, excluding the western boundary region. The ocean is divided into three parts, i.e., a constant-depth, well-mixed layer on the top, a continuously stratified moving water layer in the middle, and stagnant abyssal water at the bottom. As shown by H, a surface of no motion separates the moving water from the stagnant water. The ocean is sufficiently deep that the bottom does not interfere with the interior dynamics.

Both the southern and northern boundaries of the subpolar basin are latitudinal circles along which $w_e = 0$ and ρ_s = constant. The above assumptions guarantee that a solution with no mass exchange across these boundaries is self-consistent, thus the subpolar gyre can be studied in isolation from other gyres (Huang, 1986).

At the eastern boundary, a no-flux condition is applied. At the western boundary, potential vorticity for water particles is specified at the western boundary outflow region as a given function of Bernoulli function and density.

In the following discussion we take the base of the mixed layer as the upper surface of the interior ocean. At this surface, the Ekman pumping velocity (positive for a subpolar gyre) and the mixed layer density are specified. The density of the mixed layer, ρ_m, is assumed to be solely determined by the local atmospheric forcing, without including the interaction between the mixed layer and the water below. Assuming the mixed layer is totally passive, i.e., water is picked up by the mixed layer and transferred as Ekman flux regardless of static instability, water density at this interface, ρ_s^0, can be calculated according to boundary value problem C in H. (For the formulations of boundary value problems of the ideal-fluid thermocline, the reader is referred to H.)

Our model takes the static stability of the vertical stratification into consideration. There are two possible situations. First, $\rho_m \leqslant \rho_s^0$, water columns are gravitationally stable and the mixed layer is truly passive. Second, $\rho_m > \rho_s^0$, water columns are gravitationally unstable and convective adjustment takes place. We have made the assumption that the atmosphere has an infinite heat capacity so that convective adjustment does not change the density in the mixed layer. Therefore, the upper part of the water column, $z = [-D, 0]$, becomes totally destratified and acquires a uniform density $\rho_s = \rho_m$, see Fig. 1. Accordingly, the ocean is divided into four parts vertically, i.e., a mixed layer of constant depth and a density specified by local atmospheric forcing, a convective layer of thickness D, the unventilated thermocline with the base of the moving water at $z = -H$, and the stagnant abyssal water at the bottom. Our major interest is to study the structure of the convective layer and the unventilated thermocline.

a. Basic equations in density coordinates

We have derived basic equations in density coordinates for the ideal-fluid thermocline in H. To make this study self-contained, we include the derivation of some relevant equations.

An important dependent variable in density coordinates is the Bernoulli function defined as

$$B = p + \rho g z. \tag{1}$$

Differentiating (1) with respect to ρ gives

$$B_\rho = gz \tag{2}$$

$$B_{\rho\rho} = g z_\rho. \tag{3}$$

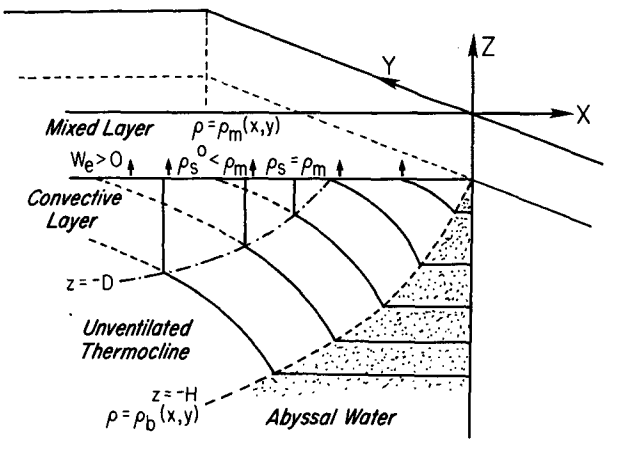

FIG. 1. Schematic of a subpolar basin. A mixed layer with constant depth is uppermost in the ocean; a convective layer is between the mixed layer and the unventilated thermocline. At the bottom is stagnant abyssal water (stippled).

Another important variable, the potential vorticity, is defined as

$$q = f\rho_z. \tag{4}$$

Substituting (4) into (3) gives

$$B_{\rho\rho} = fg/q. \tag{5}$$

This is a second-order ordinary differential equation. As has been shown by H, this equation plays a most important role in boundary value problems of the ideal-fluid thermocline.

At the upper boundary, we have two boundary conditions

$$w = w_e \quad \text{at} \quad \rho = \rho_s, \tag{6}$$

$$B_\rho = 0 \quad \text{at} \quad \rho = \rho_s, \tag{7}$$

where ρ_s has to be determined either from the specified density of the mixed layer or from the interior solution. A way of calculating the upper surface density of an ideal-fluid thermocline model, without convective adjustment, has been described by H. Denoting the upper surface density calculated from such a model as ρ_s^0, the real upper surface density is

$$\rho_s = \max(\rho_m, \rho_s^0). \tag{8}$$

Obviously, wherever $\rho_s^0 < \rho_m$, a local convective adjustment will occur, raising the density of the upper part of the water column to ρ_m.

At the base of the moving water, the dynamical fields of the moving water match that of the stagnant water continuously. Therefore, we have

$$B = B^a \quad \text{at} \quad \rho = \rho_b \tag{9}$$

$$B_\rho = B_\rho^a \quad \text{at} \quad \rho = \rho_b \tag{10}$$

where $B^a(\rho)$ and $B_\rho^a(\rho)$ are the given structure of the stagnant water, $\rho = \rho_b(x, y)$ is a free boundary determined as part of the solution.

At the eastern boundary, the no-flux boundary condition

$$u \equiv 0 \quad \text{at} \quad x = x_e \tag{11}$$

requires that

$$\rho_b = \rho_s = \rho_0 = \text{constant} \quad \text{at} \quad x = x_e. \tag{12}$$

Therefore, the thickness of the moving water is zero at the eastern boundary. This kind of eastern boundary condition introduces a singularity in the meridional velocity field near the eastern boundary, but the vertically integrated volume flux remains bounded (see H).

At the outer edge of the western boundary, potential vorticity is specified wherever water leaves the boundary

$$q = q(B, \rho), \tag{13}$$

where the function can be piecewise continuous.

To formulate a physically sound boundary value problem, we have to include the Ekman pumping condition as follows. In density coordinates, the geostrophic conditions take the forms

$$-\rho_0 fv = -B_x \tag{14}$$

$$\rho_0 fu = -B_y. \tag{15}$$

Thus, the Sverdrup relation

$$\beta v = fw_\rho/z_\rho \tag{16}$$

can be rewritten as

$$B_x = \rho_0 f^2 w_\rho/\beta z_\rho, \tag{17}$$

which upon integrating from ρ_s to ρ_b, gives

$$2\rho_0 f^2 w_e g/\beta = \int_{\rho_s}^{\rho_b} (B_\rho^2)_x d\rho. \tag{18}$$

Interchanging differentiation with integration, one obtains

$$-\int_{\rho_s}^{\rho_b} B_\rho^2 d\rho = (2\rho_0 f^2 g/\beta) \int_x^{x_e} w_e dx + \int_x^{x_e} B_\rho^2(\rho_b) d\rho_b/dx \cdot dx, \tag{19}$$

where boundary conditions (7) and (12) have been used. Equation (19) is the integral constraint applied to a boundary value problem for the ideal-fluid thermocline. In fact, this is the Sverdrup relation extended to the case of continuously stratified fluid.

b. *Solution of a uniform potential vorticity for the unventilated thermocline*

To illustrate the simplest dynamics, we study a case with a uniform potential vorticity for the whole unventilated thermocline. The cases of nonuniform potential vorticity are formulated in the Appendix. Since there is a convective adjustment process possibly involved in the problem, this uniform potential vorticity only applies before convective adjustment destroys the stratification up to a specific density value. As we will show next, the assumption of uniform potential vorticity for the unventilated thermocline reduces the problem to a simple algebraic solution with an inequality switch.

To facilitate the derivation of the relations, we replace the uniform upper part of the column with a small density gradient, thus

$$q_u = f\delta\rho/D = \epsilon \ll 1. \tag{20}$$

At the upper surface, we have

$$B = B^s, \quad B_\rho = 0 \quad \text{at} \quad \rho = \rho_s. \tag{21}$$

At the depth of $z = -D$, $\rho = \rho_s + \delta\rho$, integrating (5) gives

$$B = B^s + fg\delta\rho^2/2q_u = B^s + gD^2\epsilon/2f \approx B^s, \tag{22}$$

$$B_\rho = fg\delta\rho/\epsilon = gD. \quad (23)$$

Integrating (5) from $\rho_s + \delta\rho$ toward a high density region, one obtains

$$B_\rho = gD + fg(\rho - \rho_s)/q^h \quad (24)$$

$$B = B^s + fg(\rho - \rho_s)^2/2q^h \quad (25)$$

where

$$q^h = f_0\rho_z{}^a \quad (26)$$

is the uniform potential vorticity for the unventilated thermocline.

For the stagnant abyssal water, we have

$$B_\rho{}^a = fg(\rho - \rho_0)/q^a \quad (27)$$

$$B^a = fg(\rho - \rho_0)^2/2q^a. \quad (28)$$

Using boundary condition (10), one obtains

$$D + f(\rho_b - \rho_s)/f_0\rho_z{}^a = (\rho_b - \rho_0)/\rho_z{}^a. \quad (29)$$

The first integral in (19) can be calculated as follows:

$$\int_{\rho_s}^{\rho_b} B_\rho{}^2 d\rho = \int_{\rho_s}^{\rho_s+\delta\rho} B_\rho{}^2 d\rho + \int_{\rho_s}^{\rho_b+\delta\rho} B_\rho{}^2 d\rho. \quad (30)$$

The first integral on the right-hand side is of order ϵ; thus it vanishes as $\epsilon \to 0$. Using (24), the final result of (30) is

$$\int_{\rho_s}^{\rho_b} B_\rho{}^2 d\rho = \frac{q^h}{3fg}\{[gD + fg(\rho_b - \rho_s)/q^h]^3 - (gD)^3\}. \quad (31)$$

The second integral in (19) can be calculated by using (27)

$$\int_x^{x_e} B_\rho{}^2|_{\rho=\rho_b} d\rho_b/dx \cdot dx = -\frac{1}{3}(fg/q^a)^2(\rho_b - \rho_0)^3, \quad (32)$$

where the eastern boundary condition that $\rho_b = \rho_0$ at $x = x_e$ has been used. Therefore, the constraint (19) becomes

$$(\rho_b - \rho_0)^3 = 6\rho_0 f^3(\rho_z{}^a)^2 w_e(x_e - x)/g\beta(f - f_0) - f_0(\rho_z{}^a D)^3/(f - f_0). \quad (33)$$

Now (29, 33) are the two relations that determine the final solution. From their derivation, (29) represents the no-motion condition at the base of the moving water, while (33) is the Sverdrup relation. Suppose $D = 0$, these two relations give a solution of the ideal-fluid thermocline without convective adjustment as discussed by H.

However, for a model including convective adjustment, $\rho_s(x, y)$ calculated from these relations, with $D = 0$, may be smaller than the specified mixed layer density $\rho_m(x, y)$ from a one-dimensional air–sea interaction mixed-layer model. In such a case convective adjustment takes place, thus D is not zero and ρ_s in (29) should have been ρ_m, as specified. Thus (29, 33) become two equations for two unknown ρ_b and D. A single cubic equation for ρ_b (or D) can be derived from (29, 33) and solved directly. Other variables can be determined by corresponding equations afterward.

c. Consistent conditions for the mixed layer density

Since $D \leq 0$ for general cases, $\rho_b - \rho_0$ decreases as $|D|$ increases, from (33). As ρ_m increases gradually, the bottom of the convective layer gets closer to the base of the moving water. At the limit

$$\rho_b = \rho_s = \rho_{\lim} \quad (34)$$

i.e., the entire moving water column is vertically homogenized. From (29) one finds the depth of the convective layer for this limit case

$$D = (\rho_b - \rho_0)/\rho_z{}^a. \quad (35)$$

Substituting (34, 35) into (33), one obtains

$$\rho_{\lim} - \rho_0 = [6\rho_0 f^2 \rho_z{}^{a^2} w_e(x_e - x)/g\beta]^{1/3}. \quad (36)$$

If we denote $\rho_s{}^0$ as the upper surface density when $D = 0$, then

$$\rho_s{}^0 - \rho_0 = [(f - f_0)/f]^{2/3}[6\rho_0 f^2 \rho_z{}^{a^2} w_e(x_e - x)/g\beta]^{1/3}. \quad (37)$$

Therefore, it follows that

$$\rho_{\lim} - \rho_0 = [f/(f - f_0)]^{2/3}(\rho_s{}^0 - \rho_0). \quad (38)$$

Apparently, $\rho_{\lim} - \rho_0$ can be much larger than $\rho_s{}^0 - \rho_0$ near the southern boundary. It should be noticed that the base of the moving water in the case of no convective adjustment is located much deeper than the case corresponding to the maximum convective adjustment, $\rho_m = \rho_{\lim}$. In fact, if $D = 0$, then

$$\rho_b - \rho_0 = f[6\rho_0 \rho_z{}^{a^2} w_e(x_e - x)/g\beta(f - f_0)]^{1/3}. \quad (39)$$

As $y \to y_0$, $f \to f_0$, and if we assume w_e is linearly dependent on $(y - y_0)$, then (39) predicts a finite depth of the base of the moving water, while $\rho_{\lim} \to \rho_0$ as required by (36).

Therefore, a consistent condition for the sea surface temperature is

$$\rho_m \leq \rho_{\lim} = \rho_0 + [6\rho_0 f^2 \rho_z{}^{a^2} w_e(x_e - x)/g\beta]^{1/3}. \quad (40)$$

Within the convective adjustment region, the mixed layer density is subjected to an additional constraint. When convective adjustment takes place, the upper part of the water column at a station is totally destratified and has a constant density ρ_m. This parcel of water will not regain its original potential vorticity specified at the western boundary outflow region. In the model, we assume that this water will either maintain its density or become heavier due to further cooling. To make the mode simple, we impose a further constraint.

Within the convective adjustment region the mixed-layer density satisfies

$$\mathbf{v}_s \cdot \nabla \rho_m \geq 0, \tag{41}$$

where $\mathbf{v}_s$ is the horizontal velocity vector on the upper surface.

Because $\rho \equiv \rho_m$ within the entire depth of the convective layer, the horizontal velocity components can be calculated by integrating the thermal wind relation vertically

$$u = u_s + g\rho_{my}z/f\rho_0 \tag{42}$$

$$v = v_s - g\rho_{mx}z/f\rho_0. \tag{43}$$

Therefore, inequality is satisfied for the entire convective layer, i.e.,

$$\mathbf{v} \cdot \nabla \rho_m = \mathbf{v}_s \cdot \nabla \rho_m \geq 0. \tag{44}$$

In a word, if we specify ρ_m as subject to (41), every water particle will have its density monotonically decreased downstream.

This constraint is not essential for the model; it is chosen for convenience. Obviously, the model can be modified to keep track of the potential vorticity change due to convective adjustment and thus make this constraint unnecessary. When this constraint is satisfied, however, we do not have to keep track of all convective layers, and each station can be treated separately. Generally, this constraint has to be checked after the solution is found.

d. Sensitivity of the solution

For simplicity, our discussion here is concentrated on a model with fixed geometry and Coriolis parameter. Therefore, the external parameters remaining include the background stratification, $\rho_z{}^a$, the Ekman pumping velocity, w_e, and the imposed mixed-layer density, ρ_m. To study the sensitivity of the model, we rewrite the corresponding equations as

$$\rho_m > \rho_s{}^0 = \rho_0 + [6\rho_0(f-f_0)^2 RW(x_e - x)/g\beta]^{1/3}, \tag{45}$$

$$RD + f(\rho_b - \rho_m)/f_0 = \rho_b - \rho_0, \tag{46}$$

$$(\rho_s - \rho_0)^3 = 6\rho_0 f^3 RW(x_e - x)/g\beta(f - f_0) - f(RD)^3/(f - f_0), \tag{47}$$

where

$$RW = (\rho_z{}^a)^2 w_e, \quad RD = \rho_z{}^a D.$$

The first equation is the criterion for convective adjustment to take place. This criterion can be easily explained as follows: both strong background stratification and Ekman suction force dense isopycnals to outcrop in the subpolar gyre; meanwhile, weak Ekman suction and background stratification correspond to a warm, less dense water outcropping. Therefore, the latter case is prone to cooling on the upper surface.

It is a crude, but generally acceptable assumption to specify a mixed layer density distribution independent on the longitude. In such a case, the convective adjustment should take place first within the eastern basin where the upwelling water is much warmer and prone to cooling. In fact, deep water formation is the strongest in the northeastern corner in numerical models with similar thermal boundary condition, see Cox and Bryan (1984). However, the situation in the northern North Atlantic is much more complicated due to the salinity effect.

The sensitivity study for the model is rather complicated due to the fact that the formulation includes an inequality switch. However, Eqs. (45), (46) and (47) suggest some simple similarity solution. It is readily seen that families of solutions exist which have constant $RW = (\rho_z{}^a)^2 w_e$ and $RD = \rho_z{}^a D$, and the same mixed layer density distribution $\rho_m(x, y)$. Since RW, RD are constant, strong stratification should correspond to weak Ekman suction and shallow convective layer. Although $\rho_b(x, y)$ is the same for the whole family, the depth of the moving water for individual solutions is inversely proportional to the stratification.

3. Numerical example and discussion

We have calculated an ocean model with the northern North Atlantic in mind. The model is a rectangular basin with the following parameters:

$$L_x = 6000 \text{ km},$$

$$L_y = 3300 \text{ km},$$

$$f = f_0 + \beta y,$$

$$f_0 = 1.03 \times 10^{-4} \text{ s}^{-1},$$

$$\beta = 1.61 \times 10^{-13} \text{ cm}^{-1} \text{ s}^{-1},$$

$$w_e = 0.0001 \sin(\pi y/L_y),$$

$$\rho_z{}^a = -10^{-8} \text{ g cm}^{-4},$$

$$q^h = f_0 \rho_z{}^a,$$

where $y = 0$ is the southern boundary of the subpolar basin.

We first show three sets of maps comparing a solution having no convective adjustment with a solution corresponding to maximum convective adjustment. The first solution is the same as that determined by boundary value problem-C, as described by H; the second solution is determined by a maximum density of the mixed layer defined as

$$\rho_m \equiv \rho_{\text{lim}} = \rho_0 + [6\rho_0 f^2 \rho_z{}^{a^2} w_e (x_e - x)/g\beta]^{1/3}. \tag{48}$$

Both these solutions were first discussed by Pedlosky and Young (1983). They derived the second solution as a simple extension from the model of Luyten et al. (1983). Our model gives this solution a new physical meaning, i.e., the result of the convective adjustment process.

It is rare for the second solution to appear, unless the mixed-layer density satisfies a very specific formula (48). Nevertheless, this is a consistent solution of our model. In fact, it is readily proved that

$$\mathbf{v}_s \cdot \nabla \rho_m \equiv 0 \qquad (49)$$

is satisfied by the solution. Although some parts of the solutions have been discussed in the aforementioned papers, we include some maps to make our discussion here self-contained.

The upper surface density maps for these two cases are shown in Fig. 2. The allowable density of the mixed layer can be much larger than the upper surface density calculated from a no-convective-adjustment model, especially near the southern boundary. The allowable density of the mixed layer has a maximum at the middle of the western boundary and a minimum at the other three lateral boundaries. This result can be interpreted as an idealization of the actual sea surface temperature distribution in the northern North Atlantic.

The corresponding Bernoulli function maps are shown in Fig. 3. A major difference between these two cases is the strongly surface-intensified current in the second case, especially near the southern/northern boundaries. Apparently, surface cooling and density homogenization intensify the surface current and reduce the thickness of the moving water layer. The latter effect can be seen more clearly in the depth map of the base of the moving water in Fig. 4.

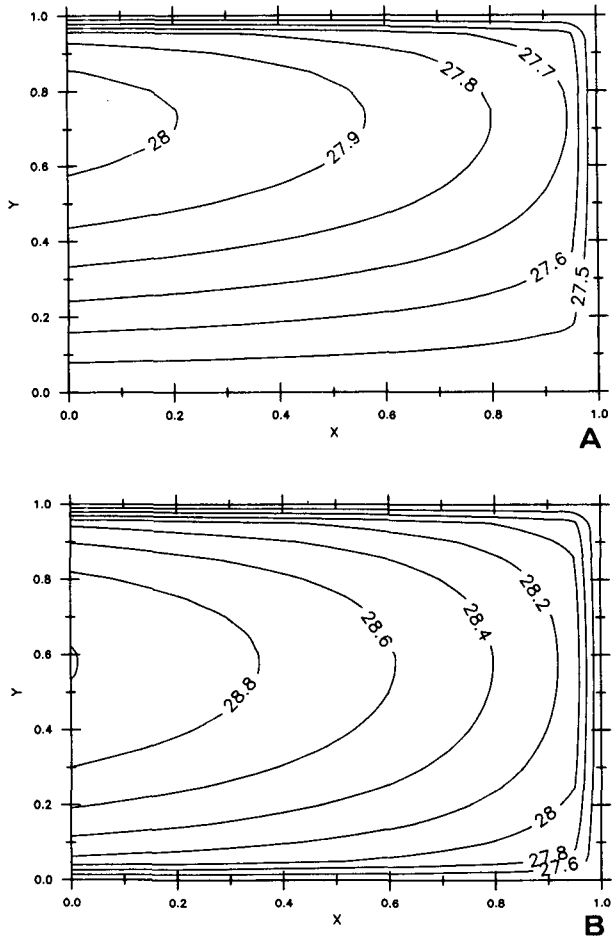

FIG. 2. Density (in units of sigma) map on the upper surface. (a) Without convective adjustment. (b) Maximum convective adjustment.

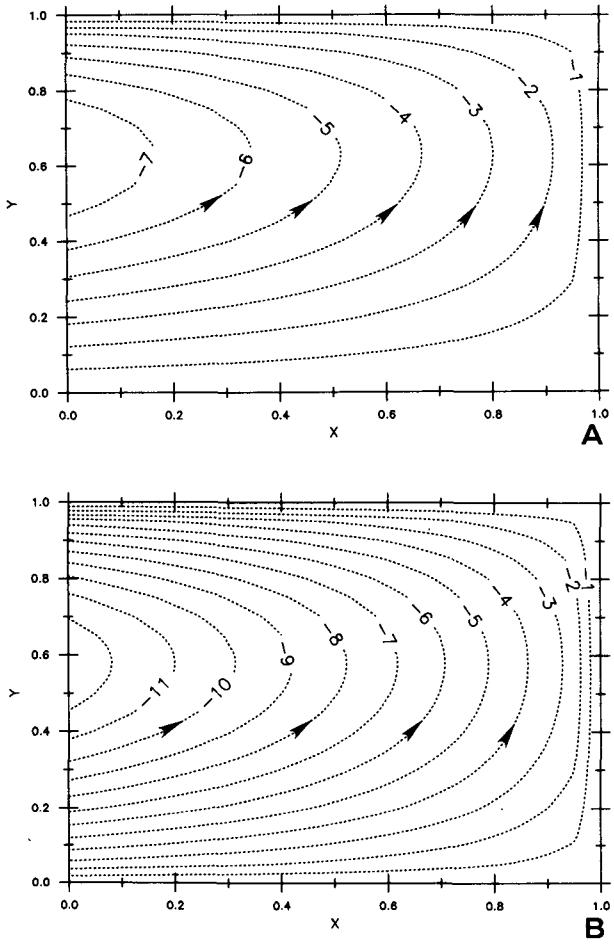

FIG. 3. Bernoulli function (in units of 10^4 g cm^{-1} s^{-2}) map on the upper surface. (a) Without convective adjustment. (b) Maximum convective adjustment.

These cases are only the two extremes for the model. Generally, the density of the mixed layer is less than that determined by (48). Our next step is to choose a density distribution in the mixed layer which satisfies constraints discussed in section 2.

We use the solution shown in Fig. 3a and choose a density distribution in the mixed layer as follows:

$$\rho = 1.0284 \quad \text{for} \quad B_s < B_{sL}$$

$$\rho = 1.0284 + (1.0284 - \rho_s^0)(B - B_{sL})/(B_{sL} - B_{sR}) \quad \text{for} \quad B_{sL} < B_s < B_{sR}$$

$$\rho = \rho_s^0 \quad \text{for} \quad B_s > B_{sR} \qquad (50)$$

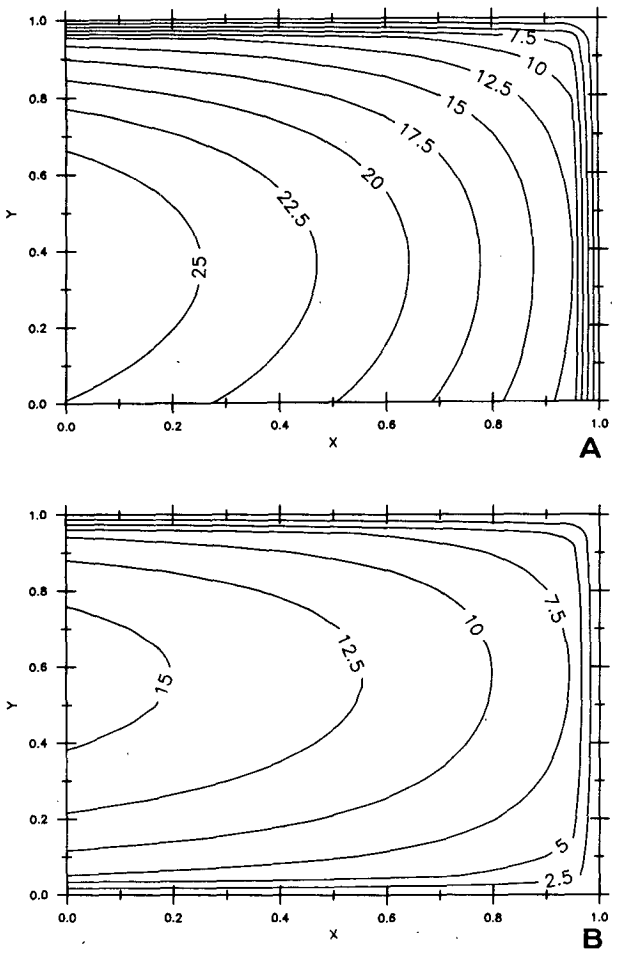

FIG. 4. The base of the moving water, in units of 100 m. (a) Without convective adjustment. (b) Maximum convective adjustment.

where

ρ_s^0 = the upper surface density shown in Fig. 2a,

$B_{sL} = -50000$ g cm^{-1} s^{-2},

$B_{sR} = -35000$ g cm^{-1} s^{-2}. (51)

Figure 5 shows this density pattern, where the dashed line corresponds to the upper surface Bernoulli function contour with the value of B_{sR} defined in (51). The density structure east of the dashed line is unessential, provided that $\rho_m \leq \rho_s^0$ is satisfied. The choice of this mixed-layer density pattern is for simplicity and self-consistency, which will be further confirmed later.

From the thermal wind relation, it is easy to see that strong horizontal surface density gradients are associated with surface-intensified currents. The western boundary currents (before and after separation) are well-known examples of these density fronts. Our model shows surface-intensified currents associated with local cooling. Although our present model is a steady model, these cooling-induced frontal structures

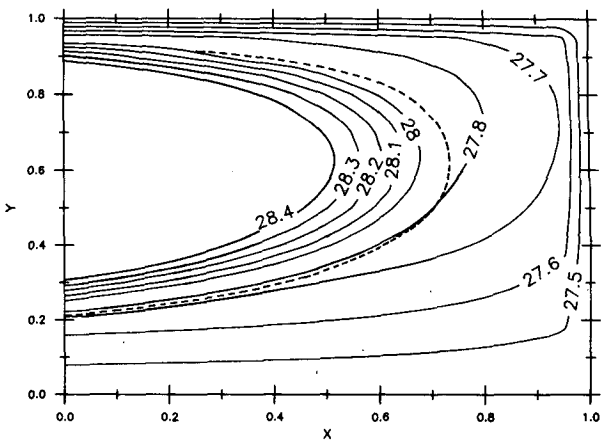

FIG. 5. Density (in units of sigma) of the mixed layer for a case with convective adjustment. East of the dashed line $\rho_m = \rho_s^0$, thus there is no convective adjustment. West of contour 28.4 density is constant.

can be visualized as a crude model for the ocean current developed in the northern North Atlantic during wintertime when cold, dry polar air masses move over the ocean. Since the surface density within this front is largely set up by the atmospheric cooling, its horizontal scale is also determined by local atmospheric forcing which simply bends the isopycnals upwards and thus creates strong frontal structure.

Because classical ideal-fluid thermocline theory excludes any mixing, it fails to describe adequately the subpolar gyre where thermal forcing is vitally important. Our model simulates the thermal forcing with a simple convective adjustment process; therefore, the essential parts of the circulation mechanisms are included.

The Bernoulli function (Fig. 6) on the upper surface shows a strong surface-intensified current along the

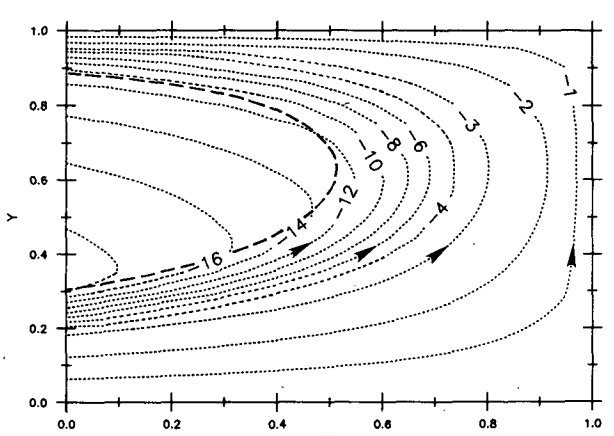

FIG. 6. Bernoulli function (in units of 10^4 g cm^{-1} s^{-2}) on the upper surface. Dashed line denotes the boundary of the constant-density region.

southern edge of the convective adjustment region. This further confirms the conclusion that cooling creates strong frontal structure near the upper surface. The dashed line indicates the outer edge of the density-homogenized area where the surface current is much weaker than at the outer edge. Near the southern, eastern, and northern boundaries, the solution is exactly the same as in Fig. 3a, because no convective adjustment takes place there. By overlaying Fig. 5 with Fig. 6, one can see that

$$\mathbf{v}_s \cdot \nabla \rho_m \geq 0$$

for this case, thus the solution is self-consistent.

The depth of the convective layer is shown in Figure 7, where the short-dashed line represents the eastern edge of the convective area, $D = 0$, and the long-dashed line indicates the outer edge of the constant density region of the mixed layer. Apparently, the long-dashed line is the same as the maximum depth line (some discrepancy is due to the smoothing process in the contour graphic routine). West of this line, the bottom of the convective layer gradually rises due to Ekman suction.

The depth map of the base of the moving water is shown in Fig. 8, where the short-dashed line represents the outer edge of the convective region. East of this line the solution is the same as in Fig. 4a. The long-dashed line indicates the outer edge of the constant density region of the mixed layer. As in Fig. 7, one sees the strongest distortion of the map near this line.

The last two figures, 9 and 10, show the density sections at the central latitude ($y = 0$, Fig. 9) and the western boundary ($x = 0$, Fig. 10). These two maps show three major domains in the circulation. First, there is a convective layer on the top where the isopycnals are vertical and there is even an entirely density-homogenized area in the upper left corner of Fig. 9 and the upper central part of Fig. 10. Second, there

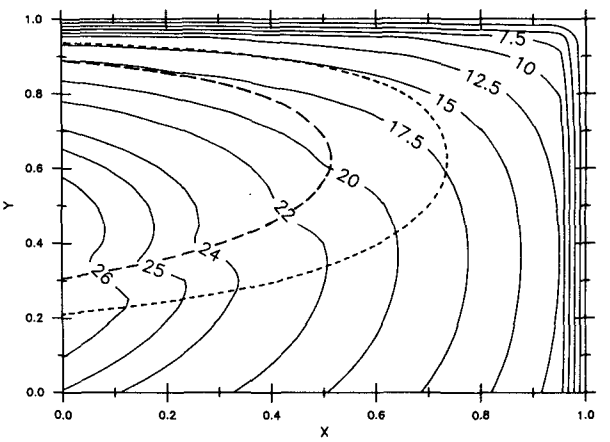

FIG. 8. The base of the moving water in units of 100 m. Short-dashed line is the outer edge of the convective zone. Long-dashed line is the edge of the region of constant surface density.

is an unventilated thermocline below the upper surface or the convective layer; water in this layer has a uniform potential vorticity specified as a given boundary condition. Finally, there is the stagnant abyssal water next to the eastern boundary and below the moving unventilated thermocline. The base of the moving water separates the abyssal water from the moving water (dashed line in Figs. 9 and 10).

In the example above we have assumed that the density of the mixed layer is constant within a larger area near the western boundary, see Fig. 5. In fact, if we impose the same density forcing only around the edge of the same area but with lighter surface water *inside* this area, the same solution is still valid. Since the upper part of the water column is destratified at the edge of this area, this homogeneous water will keep its upward cyclonic motion until it is picked up by the mixed layer.

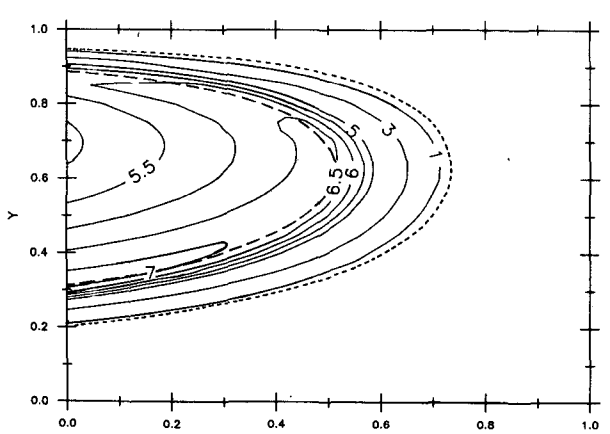

FIG. 7. Depth (in units of 100 m) of the convective layer. Short-dashed line denotes the outer edge, $D = 0$, and the long-dashed line denotes the edge of the constant-density region.

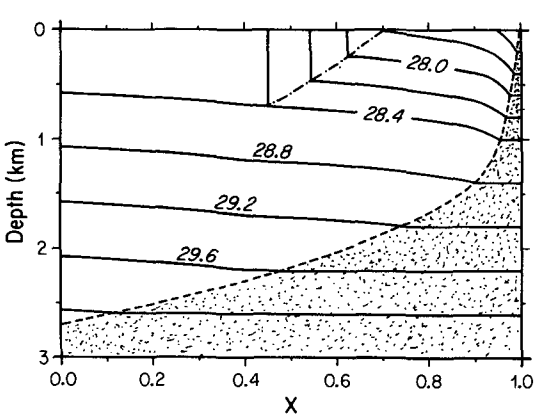

FIG. 9. Density profile at $y = 0.5$. Dot-dashed line is the bottom of the convective layer where isopycnals are vertical. Water in the upper-left corner has a uniform density. Contour interval doubles below $\sigma_\theta = 28.4$. Stippled area denotes the stagnant abyssal water.

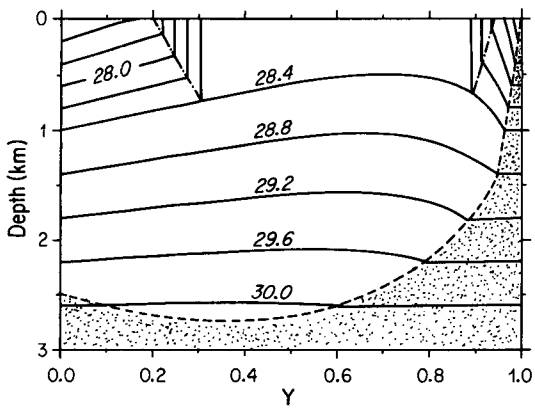

FIG. 10. Density profile at the western boundary. See explanation for Fig. 9.

4. Conclusion

We have extended the ideal-fluid thermocline theory by including a weakly convective adjustment in a subpolar basin. Where the mixed layer is subjected to strong cooling and evaporation, water in this layer becomes heavier than the water below and convective adjustment takes place. Convective adjustment destratifies the upper part of the water column and creates a homogeneous water layer. As a result of these cooling and mixing processes, the current becomes more surface-intensified and the moving water stratum is shallower. Around the edge of a strong surface cooling area there is a density frontal structure with its associated surface-intensified current.

The model is a simple extension of the classical ideal-fluid thermocline model in which water particles conserve their properties. Although the model reproduces some features similar to the observed structure in the oceans, its application is limited by the major assumptions made in the model.

First, the density of the mixed layer is calculated without including the contribution of the interaction with water below (upwelling, mixing). Consequently, the model tends to overestimate the density of the mixed layer and the effect of the convective adjustment.

Second, the constraint that the mixed layer density must be less than certain values imposed by other parameters in the model seriously limits the applicable range of the model, especially in the northern part of the subpolar gyre.

Third, probably, the strongest limitation is the assumption of a constant surface density along the eastern boundary. Although this condition simplifies the model greatly, it seems quite different from the real ocean. In fact, due to strong cooling in the subpolar basin, the sea surface temperature along the eastern boundary cannot be constant at all. A more realistic model should have a variable sea surface density along the eastern boundary and thus a nonzero zonal velocity at the boundary.

These major deficiencies in the model should be improved in further study. Since thermal forcing plays an important role in the North Atlantic, only a model which takes thermohaline circulation into account can provide realistic solutions to the problem. The present model is only a first step toward this goal.

Acknowledgments. The basic idea in this study was formulated while the author visited the University of California at Los Angeles in December 1986. He is indebted to Prof. Michael Ghil for his gracious hospitality. This work has been supported by a Mellon Advanced Study Award from the Woods Hole Oceanographic Institution and a grant from the National Science Foundation (OCE86-14771).

APPENDIX

A Boundary Value Problem for General Cases

For cases of nonuniform potential vorticity for the unventilated thermocline, the subpolar gyre circulation with weakly convective adjustment can be formulated as:

Boundary value problem D

Equation (5) with the following boundary conditions constitute a deterministic two-point boundary value problem with inequality constraint,

$$B_{\rho\rho} = fg/q(B, \rho) \tag{5}$$

$$B_\rho \leqslant 0 \quad \text{at} \quad \rho = \rho_s \geqslant \rho_m \tag{A1}$$

$$B = B^a(\rho_b) \quad \text{at} \quad \rho = \rho_b \tag{9}$$

$$B_\rho = B_\rho{}^a(\rho_b) \quad \text{at} \quad \rho = \rho_b \tag{10}$$

$$-\int_{\rho_s}^{\rho_b} B_\rho{}^2 d\rho = (2\rho_0 f^2 g/\beta) \int_x^{x_e} w_e dx + \int_x^{x_e} B_\rho{}^2(\rho_b) d\rho_b/dx \cdot dx. \tag{19}$$

Here the potential vorticity, $q = q(B, \rho)$, for all unventilated thermoclines is a given function (it is not necessarily continuous), $B^a(\rho)$ and thus $B_\rho{}^a(\rho)$ are given functions, $\rho_m = \rho_m(x, y)$ is the given density distribution in the mixed layer determined from local atmospheric forcing. Both ρ_s and ρ_b are free boundaries of the problem. Therefore, this is a boundary value problem of a second-order ordinary differential equation with two free boundaries, an inequality constraint at one free boundary, and an integral constraint which includes integrals in both the ρ- and x-coordinates.

For other boundary value problems of the ideal-fluid thermocline, i.e., boundary value problems A, B and C, the reader is referred to H. There is one common characteristic of all four of these boundary value problems; they always reduce the task of solving the original high-order partial differential equation to repeatedly

solving some free boundary value problems of a simple second-order ordinary differential equation.

Since the convective adjustment process is involved in the problem, the potential vorticity of the upper part of a water column is actually zero. Therefore, (13) is only valid for the water particle before convective adjustment destratifies the upper column.

A further assumption is made that

$$\rho_m \leqslant \rho_0 \quad \text{at} \quad x = x_e,$$

which is required for the self-consistency of the solution, although this constraint can be released if the constant density condition along the eastern boundary is changed. Therefore, the integration of boundary value problem D can be started from the eastern boundary and carried out westward as follows:

The subpolar basin is divided into several latitudinal sections along which the integration can be carried out independently.

At each latitudinal section, the integration progresses westward station by station. At each station boundary value problem D is solved by a shooting method (or other numerical methods). First, an initial guess of ρ_b is chosen. Using (9, 10) both B and B_ρ can be calculated, and thus Eq. (5) can be integrated from $\rho = \rho_b$ toward $\rho = \rho_m$. The integration stops either at $\rho = \rho_s > \rho_m$ with $B_\rho = 0$ satisfied or at $\rho = \rho_m$ with the inequality $B_\rho < 0$ satisfied. Therefore, only one inequality in (A1) will be satisfied, i.e.,

$$B_\rho = 0 \quad \text{at} \quad \rho = \rho_s > \rho_m$$

or

$$B_\rho < 0 \quad \text{at} \quad \rho = \rho_m.$$

Second, the integration constraint (19) is checked to see whether the initial guess of ρ_b gives a satisfactory solution. Since the first few guesses of ρ_b are unlikely to give the correct solution, ρ_b is repeatedly adjusted until (19) is met.

Solving the boundary value problem with a shooting method is relatively easy to program. However, skillful numerical testing and examination are required to make sure that the program does converge to a physically sound solution.

REFERENCES

Cox, M., and K. Bryan, 1984: A numerical model of the ventilated thermocline. *J. Phys. Oceanogr.*, **14,** 674–687.

Huang, R. X., 1986: Solutions of the ideal-fluid thermocline with continuous stratification. *J. Phys. Oceanogr.*, **16,** 39–59.

——, 1988: On boundary value problems of the ideal-fluid thermocline. *J. Phys. Oceanogr.*, **18,** 619–641.

Luyten, J. R., J. Pedlosky and H. Stommel, 1983: The ventilated thermocline. *J. Phys. Oceanogr.*, **13,** 292–309.

Pedlosky, J., and W. R. Young, 1983: Ventilation, potential vorticity homogenization and the structure of the ocean circulation. *J. Phys. Oceanogr.*, **13,** 2020–2037.

Rhines, P. B., and W. R. Young, 1982: A theory of the wind-driven circulation. I. Mid-ocean gyres. *J. Mar. Res.*, **40**(Suppl.), 559–596.

Robinson, A. R., and H. Stommel, 1959: The oceanic thermocline and the associated thermohaline circulation. *Tellus,* **3,** 295–308.

Welander, P., 1959: An advective model of the ocean thermocline. *Tellus,* **11,** 309–318.

——, 1971: Some exact solutions to the equations describing an ideal-fluid thermocline. *J. Mar. Res.*, **29,** 60–68.